Applied Thermal Engineering 103 (2016) 47–55

Contents lists available at ScienceDirect

Applied Thermal Engineering

journal homepage: www.elsevier.com/locate/apthermeng

Research Paper

Measuring the average volumetric heat transfer coefficient of a liquid–liquid–vapour direct contact heat exchanger

Ali Sh. Baqir [a], Hameed B. Mahood [b,*], Alasdair N. Campbell [c], Anthony J. Griffiths [d]

[a] Najaf Technical College, Department of Aeronautical Engineering, Iraq
[b] University of Misan, Misan, Iraq
[c] University of Surrey, Department of Chemical and Process Engineering, UK
[d] University of Cardiff, Department of Mechanical, Manufacturing and Medical Engineering, UK

HIGHLIGHTS

- Measurements of U_v in a 3-phase spray column DCHE.
- Effect of Q_c, Q_d, D_o, H_v and sparger configuration was examined.
- U_v decreases with D_o and H_v.
- U_v increases with increasing continuous and dispersed phase flow rates.
- Very slight effect of sparger configuration on U_v.

ARTICLE INFO

Article history:
Received 11 February 2016
Accepted 16 April 2016
Available online 19 April 2016

Keywords:
Three-phase direct contact exchanger
Volumetric heat transfer coefficient
Sparger configuration
Heat transfer measurement

ABSTRACT

The average volumetric heat transfer coefficient in a spray column liquid–liquid–vapour direct contact evaporator has been experimentally investigated. The experiments were carried out utilising a cylindrical Perspex tube of diameter 10 cm and height and 150 cm. Saturated liquid *n*-pentane and warm water at 45 °C were used as the dispersed and continuous phases, respectively. Three different dispersed flow rates (10, 15 and 20 L/h) and four different continuous phase flow rates (10, 20, 30 and 40 L/h) were used in the study. The effect of different parameters, such as the initial drop size, continuous and dispersed phase flow rates and sparger configuration, on the average volumetric heat transfer coefficient in the evaporator was studied. The results showed that the average volumetric heat transfer coefficient was reduced as the initial drop size increased. Also, both the continuous phase and the dispersed phase flow rates have a significant positive impact on the average volumetric heat transfer coefficient.

1. Introduction

The efficient design of an energy conversion system requires the extraction of the maximum thermodynamic potential of the energy source. This process is carried out by the heat exchanger, where the thermal energy transfers between two different fluid streams. Heat exchangers can be split into two main types: surface types, such as the shell and tube heat exchanger and direct contact heat exchangers, for example, the spray column.

In surface type exchangers, the two fluid streams (hot and cold), are completely separated by a solid barrier through which heat is transferred. Therefore, the ability of this type of exchanger to extract the thermodynamic potential energy is constrained by the heat transfer resistance of the surface. This surface is also exposed to fouling, corrosion and thermal stresses, especially when the exchanger operates over a large temperature range. Practically, such problems are alleviated by different technologies, e.g. using a chemical as a corrosion inhibitor, which raises the operational cost, or the use of more expensive materials of construction, which raises the capital cost. This, of course, hinders the applicability of surface type heat exchangers in low-temperature processes. The capital cost of a traditional surface type exchanger is also high due to the large surface area required to overcome the low heat transfer rate or heat transfer coefficient. The operational cost is high mainly due to the expense of continuous maintenance, fouling and corrosion. These problems and others could be solved by using the second type of heat exchanger i.e. the direct contact heat exchanger. These exchangers bring the fluid streams into direct physical contact and therefore eliminate the need for physical

* Corresponding author.
E-mail address: hbmahood@yahoo.com (H.B. Mahood).

http://dx.doi.org/10.1016/j.applthermaleng.2016.04.067
1359-4311/

Nomenclature

A	cross-sectional area of column, m^2
C_{pc}	specific heat of continuous phase, kJ/kg °C
h_{fg}	latent heat of condensation, kJ/kg
$\dot{m}_d$	dispersed phase mass flow rate, kg/min
$\dot{m}_c$	continuous phase mass flow rate, kg/min
$\dot{m}_v$	dispersed (vapour) mass flow rate, kg/min
Q	heat transfer rate, kW
T	temperature, °C
ΔT_{lm}	log-mean temperature difference, °C
U	velocity of continuous phase, m/s
ΔZ	sub-height along column, m

Subscripts

c	continuous phase
d	dispersed phase
i	initial, or location
o	outlet

barriers. This elimination means that a direct contact heat exchanger has many advantages over the surface type heat exchanger. In practice, it has a very high heat transfer coefficient, especially when it utilises a phase change. Also, there is much less corrosion and fouling and it can be operated with a very low-temperature difference [1]. Therefore, it can be used in different industrial applications, such as water desalination, solar energy applications and power production from low-grade energy resources such as geothermal energy, where surface type heat exchangers are rendered uneconomic [2]. Nevertheless, the direct contact heat exchanger has several obstacles to implementation. The most important are: the two fluid streams must be immiscible to avoid intimate mixing between them, which could be extremely expensive if later purification of the contaminated stream is necessary. Secondly, the two streams must be at the same pressure, which is not a requirement of surface type exchangers.

Only limited attention has been paid to understanding the effective parameters which control the performance of the liqui d–liquid–vapour direct contact evaporator. Most of these studies are theoretical, and they concentrate on the temperature distribution along the evaporator and the volumetric heat transfer coefficient. Bauerle and Ahlert [3] studied the volumetric heat transfer coefficient and the holdup ratio of an evaporative spray column direct contact heat exchanger, experimentally. They observed a linear relationship between the volumetric heat transfer coefficient and hold-up ratio, up to a holdup 60%. Beyond this value, the volumetric heat transfer coefficient increased rapidly towards the flooding point and then decreased. The same trend in the variation of volumetric heat transfer coefficient with the column holdup ratio was also found experimentally and correlated by Plass et al. [4]. They concluded that their correlations are an accurate prediction of the volumetric heat transfer coefficient of the direct contact spray column heat exchanger, and they could be used successfully for design or sizing.

Many investigators have pointed out that the volumetric heat transfer coefficient, the holdup ratio and the heat transfer rate are affected strongly by the dispersed phase flow rate, while the continuous phase has no significant impact (e.g., [5–9]). An inverse effect of the initial drop diameter on the average volumetric heat transfer coefficient was observed experimentally by Sideman et al. [10].

Siqueiros and Bonilla [6] illustrated promising results when they studied the inlet and the outlet temperatures of both the dispersed (pentane) and the continuous phases (water) during the direct contact evaporation process. They observed that when the initial temperature (inlet temperature) of the continuous phase ranged between 75 and 88 °C and the inlet temperature of the dispersed phase between 23 and 38 °C, the continuous phase outlet temperature was between 70 and 84 °C and the dispersed phase outlet temperature between 72 and 85 °C. Battya et al. [11] numerically studied the temperature distribution of both the continuous and the dispersed phases along the direct contact evaporator. A general numerical solution was carried out by Core and Mulligan [12], Summers and Crowe [13] and Brickman and Boehm [14]. They investigated the temperature distribution along the height of a direct contact spray column evaporator. Brickman and Boehm [14] concentrated on the possibility of maximising the three-phase, direct contact heat exchanger output by solving the one-dimensional, continuity, momentum and energy equations using a Runge–Kutta technique. Birkman and Boehm's [14] results revealed that the optimal performance is achieved when the dispersed phase is injected at its saturation temperature. Similarly, Coban and Boehm [15] and Jacobs and Golafshani [16] predicted the temperature distribution of the dispersed and the continuous phase along the column height. Tadrist et al. [17] developed a numerical solution including the coalescence of the evaporating drops and carried out experimental measurements of the temperature distribution and holdup ratio in the liquid–liquid–vapour direct contact spray column evaporator.

Analytical models describing a liquid–liquid–vapour heat exchanger are very rare because of the many complex interacting phenomena. In this context, and based on an expression for the heat transfer coefficient for a single drop evaporating in an immiscible liquid developed previously [18], an analytical solution for the local and the average heat transfer coefficient for multiple drops evaporating in a spray column direct contact heat exchanger was developed by Mori [19]. Recently, Mahood et al. [20] have derived analytically the temperature distribution of both continuous and dispersed phases along a three-phase direct contact evaporator. Most recently, Wang et al. [9] accurately measured the interface temperature of the continuous phase, and accordingly they calculated the heat transfer coefficient of *n*-pentane drops evaporating in direct contact with hot water. The temperature driving force for evaporation was accordingly the difference between the interface temperature and the drop saturation temperature. They concluded that the value of the heat transfer coefficient calculated based on the interface temperature was significantly greater than that calculated using the continuous phase temperature. Jiang et al. [21] observed that the effective height of the direct contact evaporator is reduced by up to 25% when using packing material, under temperature differences less than 8 °C. Also, a significant increase in the associated volumetric heat transfer coefficient was recorded.

Finally, Mahood et al. [1,2,23–25] have investigated the heat transfer characteristics of the vapour–liquid–liquid direct contact condenser both experimentally and theoretically. In general, the mass flow rate ratio was noted to have a significant impact on the direct contact heat transfer process with no considerable effect from the initial temperature of the dispersed phase. An increase in the temperature (both transient and steady state) of the continuous phase with height was observed experimentally and predicted analytically [2,22]. Also, the volumetric heat transfer coefficient

during transient and steady state condenser operation was measured [23,24]. The thermal efficiency of the condenser and accordingly the condenser cost were also evaluated and compared with the shell and tube condenser [1]. A relatively high efficiency with a low mass flow rate ratio and a significantly lower cost were noted. Furthermore, the flow limitation due to flooding and the associated volumetric heat transfer coefficient of the three-phase direct condenser were evaluated experimentally [25].

In the present study, measurement of the average volumetric heat transfer coefficient within the liquid–liquid–vapour direct contact evaporator was carried out. The effects of the continuous phase mass flow rate, the dispersed phase mass flow rate, the sparger configuration and the initial drop diameter on the volumetric heat transfer coefficient were examined.

2. Experimental setup and procedure

Fig. 1a shows the experimental rig used in the present study. It consists of three main parts: the test section (direct contact evaporator), the continuous phase supply system and the dispersed phase supply system. The test section is a 150 cm long Perspex tube with a 10 cm internal diameter. Twenty holes were made along the column, which were used to fix 20 calibrated K-type thermocouples (inaccuracy ±1 °C). The distance between each thermocouple is 7.5 cm. The test section is connected to the dispersed phase supply at the bottom via a sparger. The continuous phase inlet tube is at the top of the test section. Three different sparger configurations, with the same nozzle diameter (7 nozzles, 19 nozzles and 36 nozzles) were implemented throughout the experiments (see Fig. 1b).

The continuous phase supply system is comprised of a large constant temperature water bath with a controller, water pump, pipes, fittings and valves. The water bath capacity is 500 L, and it is heated by three electric heaters (3 kW each). A pressure safety valve (set to 1.5 bar) is used to control the pressure in the water bath. Distilled water was used as a continuous phase fluid. It is supplied from a large storage tank (5 m^3) via copper tubing and heated using a 10 mm outer diameter 2.5 m long copper coil, which is completely immersed in the constant temperature water bath. The coil is connected to a 4.8 mm inside diameter, and 1.6 mm bore silicone tube that is used to pump the hot water via a peristaltic pump (30 L/h maximum flow rate) to the test section. The water flow rate was measured before entering the test section using a rotameter (±1.5% inaccuracy).

The dispersed phase supply system consists of a plastic 20 L capacity storage tank, peristaltic pump, pipes, fittings and valves. Liquid *n*-pentane was used as a dispersed phase because it exhibits a high net cycle efficiency, very low fluid losses and relatively low turbine costs.

Its properties appear in Table 1. The mass flow rate of the dispersed phase (*n*-pentane) and its temperature are measured using a rotameter and a calibrated thermocouple just before injection into the test section.

Twenty calibrated K-type thermocouples are used to measure the temperature distribution along the test section, including the inlet and outlet of both phases. These thermocouples are connected to a digital data logger and PC. Also, a surface coil type condenser is used to condense the dispersed phase vapour produced at the top of the test section.

The experiments began with the preparation of the continuous phase by heating the water to the desired temperature using the water bath. It was then injected directly into the test section from the top. Its temperature and flow rate were measured. The hot water was circulated throughout the test section to maintain a constant temperature in the test section. The dispersed (*n*-pentane liquid) phase was then injected by the peristaltic pump into the bottom of the test section via the sparger. The temperature and flow rate of the dispersed phase were measured.

Dispersed liquid pentane drops were formed at the sparger. These drops rose in the column due to the buoyancy force. Thereafter, a direct counter-current contact between the dispersed phase and the continuous phase took place along the column.

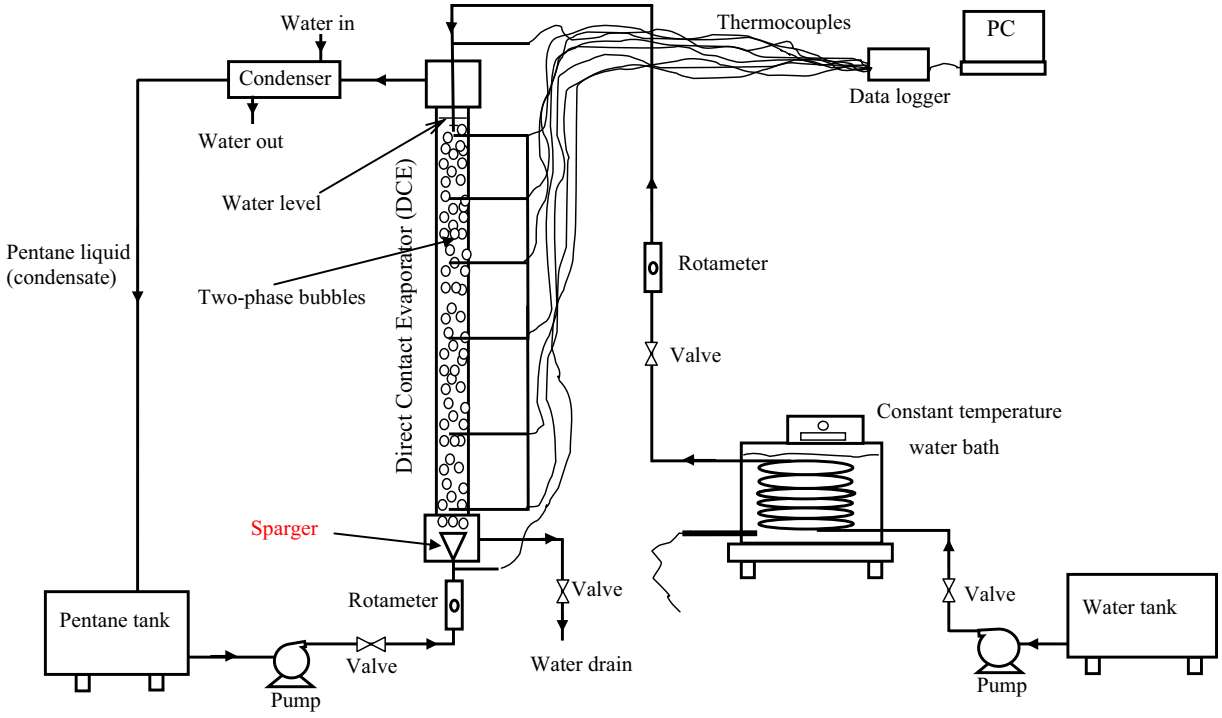

Fig. 1a. Schematic diagram of the experimental rig.

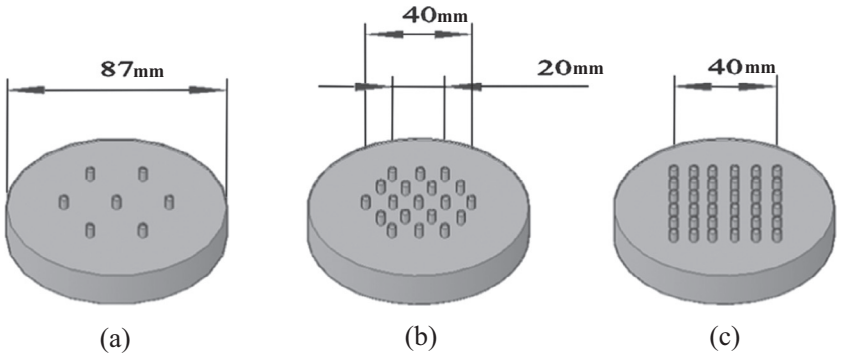

Fig. 1b. Sparger configurations, (a) 7 holes, (b) 19 nozzles and (c) 36 nozzles.

Table 1
The physical properties of *n*-pentane at 1 bar and saturation temperature.

Property	Values
Saturation temperature (°C)	36.0
Molar mass (kg/kmol)	72.15
Thermal diffusivity (m^2/s)	7.953×10^{-8}
Specific heat of liquid (kJ/kg K)	2.363
Specific heat of vapour (kJ/kg K)	1.66
Thermal conductivity of liquid (W/m K)	0.1136
Thermal conductivity of vapour (W/m K)	0.015
Kinematic viscosity (m^2/s)	2.87×10^{-7}
Viscosity (kg/m s)	1.735×10^{-4}
Latent heat of vaporisation (kJ/kg)	359.1
Density of liquid (kg/m^3)	621
Density of vapour (kg/m^3)	2.89
Surface tension (N/m)	0.01432

Due to the temperature difference between the two phases, the dispersed drops absorbed the heat from the continuous phase and evaporated as they moved up the column. The temperatures of the continuous phase along the column height were measured and directly displayed on the PC. Two-phase bubbles were observed along almost the entire height of the column, which is consistent with e.g. [14,26]. The pentane evaporated completely before the bubbles reached the top surface of the water; the section of the column over which the phase change occurred is termed the active height. After the pentane was evaporated, there remained a driving force for heat transfer to the bubbles, and so the vapour collected at the top of the column was in fact slightly superheated. The superheated vapour was collected and condensed using a surface type condenser and returned to the liquid pentane storage tank. The operational conditions of the experiments can be seen in Table 2.

3. Results and discussion

To calculate the average volumetric heat transfer coefficient in the three-phase direct contact heat exchanger, the column height was divided into seven equal sub-volumes. An energy balance over each individual sub-volume was performed based on the following assumptions:

Table 2
Conditions of experimental operations.

Inlet water temperature	Inlet dispersed temperature	Pressure at top of pipe	Water volume flow rate	*n*-pentane volume flow rare
45 °C	36 °C	1 atm	10–40 L/h	10–20 L/h

- Latent heat is dominant during the process; therefore, the effect of sensible heat can be neglected.
- The dispersed phase (liquid pentane drops) enters the heat exchanger at its saturation temperature, which is constant along the direct contact heat transfer process (i.e. the effect of hydrostatic pressure variation is ignored).
- No heat losses from the direct contact heat exchanger to the environment.
- The continuous and dispersed phase flow rates are constant because there is no mixing between them throughout the column height. Also, there is a constant hold-up along the exchanger [16].

Using the first assumption above, the energy balance over a sub-volume of the liquid–liquid–vapour heat exchanger can be written as [27]:

$$Q_i = \dot{m}_c C_{pc}(T_{co} - T_{ci})_i = \dot{m}_{di} h_{fg} \tag{1}$$

where T_{ci} and T_{co} represent the temperature of the continuous phase as it enters and leaves the sub-volume, respectively.

The volumetric heat transfer coefficient is obtained as:

$$U_{vi} = \frac{Q_i}{A\Delta Z_i (\Delta T_{lm})_i} \tag{2}$$

where $(\Delta T_{lm})_i$, Q_i, A, $\dot{m}_c$, $\dot{m}_{di}$ and ΔZ_i denote the log-mean temperature difference for each sub-volume, the total heat transfer rate for each sub-volume, the direct contact condenser cross-sectional area, the continuous phase mass flow rate, the dispersed mass flow rate that condenses in the sub-volume and the height of a sub-volume, respectively.

To avoid the uncertainty in the temperatures that arises due to backmixing and non-linear drop size and distribution in the column, the log-mean temperature difference is used, as:

$$\Delta T_{lm} = \frac{(T_{ci} - T_{co})}{\ln\left(\frac{T_{ci} - T_d}{T_{co} - T_d}\right)} \tag{3}$$

Combining Eqs. (1)–(3) yields the volumetric heat transfer coefficient:

$$U_{vi} = \frac{\dot{m}_c C_{pc}}{A \cdot \Delta Z_i} \ln\left[\frac{(T_{co} - T_d)_i + \left(\frac{\dot{m}_{di}}{\dot{m}_c}\right)\frac{h_{fg}}{C_{pc}}}{(T_{co} - T_d)_i}\right] \tag{4}$$

where C_{pc}, T_d, T_{co} and h_{fg} denote specific heat of the continuous phase, the temperature of the continuous phase at each individual sub-volume outlet, the temperature of the dispersed phase at each individual inlet sub-volume (saturation temperature) and the latent heat of condensation, respectively.

The amount of dispersed phase mass flow rate evaporated in each sub-volume can be calculated as:

$$\dot{m}_{di} = \frac{Q_i}{h_{fg}} \quad (5)$$

Different effective parameters such as the initial drop size, the continuous phase mass flow rate, the dispersed phase flow rate, the hold-up and the continuous active height on the average volumetric heat transfer coefficient have been studied experimentally. The effects of these parameters are discussed, in turn, below.

3.1. Effect of initial drop size and sparger configuration

It was noted earlier that the volumetric heat transfer coefficient in a spray column direct contact evaporator is inversely affected by the initial diameter of the drops of the dispersed phase [10]. However, few experimental data [10] and limited theoretical evidence [14–16] describing this relationship are available.

Fig. 2 shows the variation of the average volumetric heat transfer coefficient with initial drop diameter for different continuous phase volumetric flow rates and three different sparger configurations. Experimentally, the average initial drop size was measured using FastCam SA1.1 Ultra High-Speed Video camera (up to 65,000 fps).

In general, the average volumetric heat transfer coefficient decreases with an increase in initial drop diameter, which agrees with previous theoretical findings [e.g. 5,16,19] and experimental data [10]. Clearly, when the initial drop diameter is small, for a given flow rate, the total interfacial heat transfer area will be large, and consequently more heat transfer between the two phases will take place. Also, the probability of coalescence of the small bubbles is low in comparison with large drops. Coalescence tends to reduce the active interfacial heat transfer area, which is reflected in the average volumetric heat transfer coefficient of the evaporator [21].

Simultaneously, the figures clearly illustrate a rise in the average volumetric heat transfer coefficient, over the entire range of drop size considered, as the continuous phase flow rate is increased. The higher continuous phase flow rate increases the energy source in the evaporator, and hence enhances the heat transfer. This is primarily as a result of maintaining a large temperature driving force for heat transfer. The energy removal from the continuous phase results in a small temperature decrease when the flow rate is high. It is also conceivable that the higher continuous phase flow rate might result in a smaller drop rise velocity due to the large drag force on the drops as they move along the column. In addition, the figure reveals there is no effect of the continuous phase flow rate on the average initial drop size.

Sparger configuration is another factor that could affect the heat transfer performance of the direct contact heat exchanger. It is responsible for the initial size and distribution of the drops, which affect the heat exchange process in the heat exchanger, as shown above.

Three different sparger configurations, with the same nozzle diameter were studied; 7, 19 and 36 nozzles (see Fig. 1b), have been tested through the experiments. Fig. 3 illustrates the variation of the average of the volumetric heat transfer coefficient with the sparger configuration for four different continuous phase flow rates. Surprisingly, the results revealed that for a constant dis-

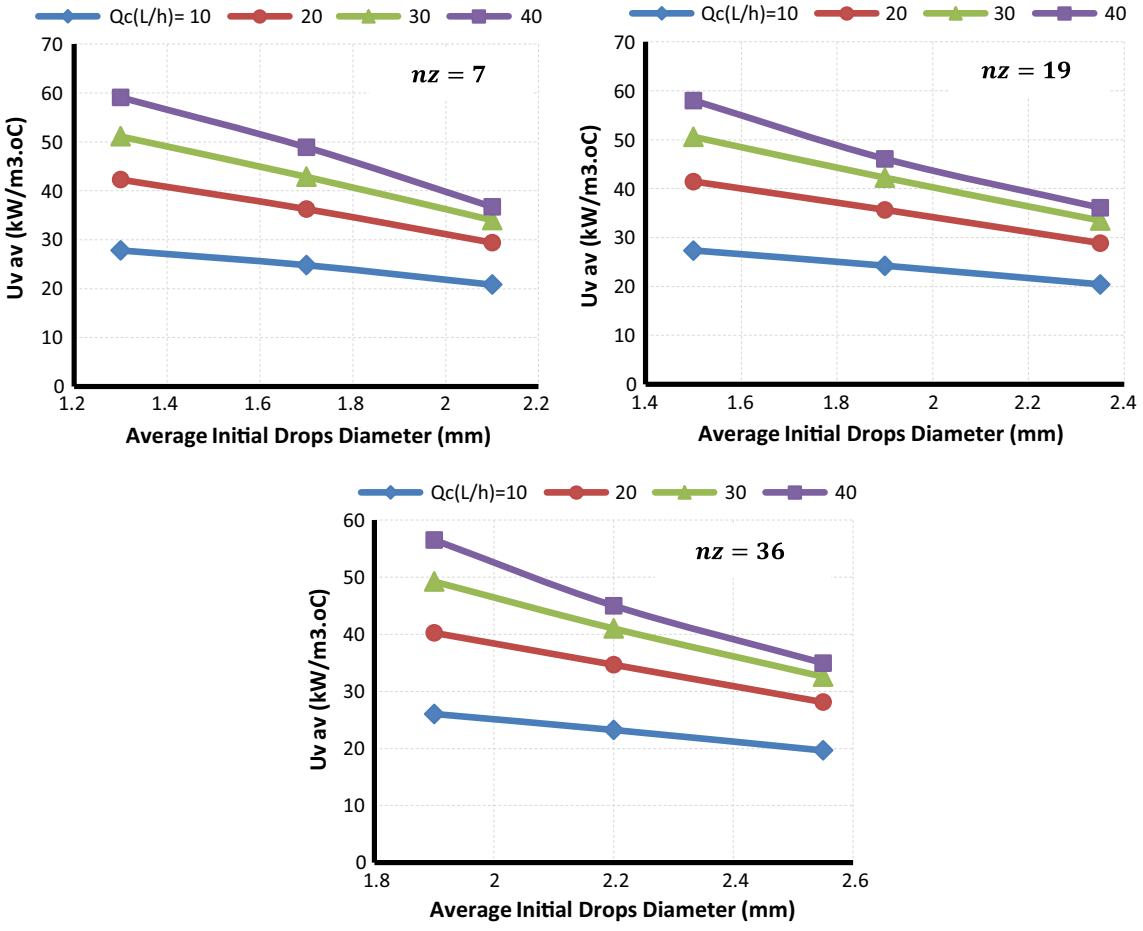

Fig. 2. Variation of the average volumetric heat transfer coefficient with average initial drop diameter for four different continuous volumetric flow rates and three different sparger configurations.

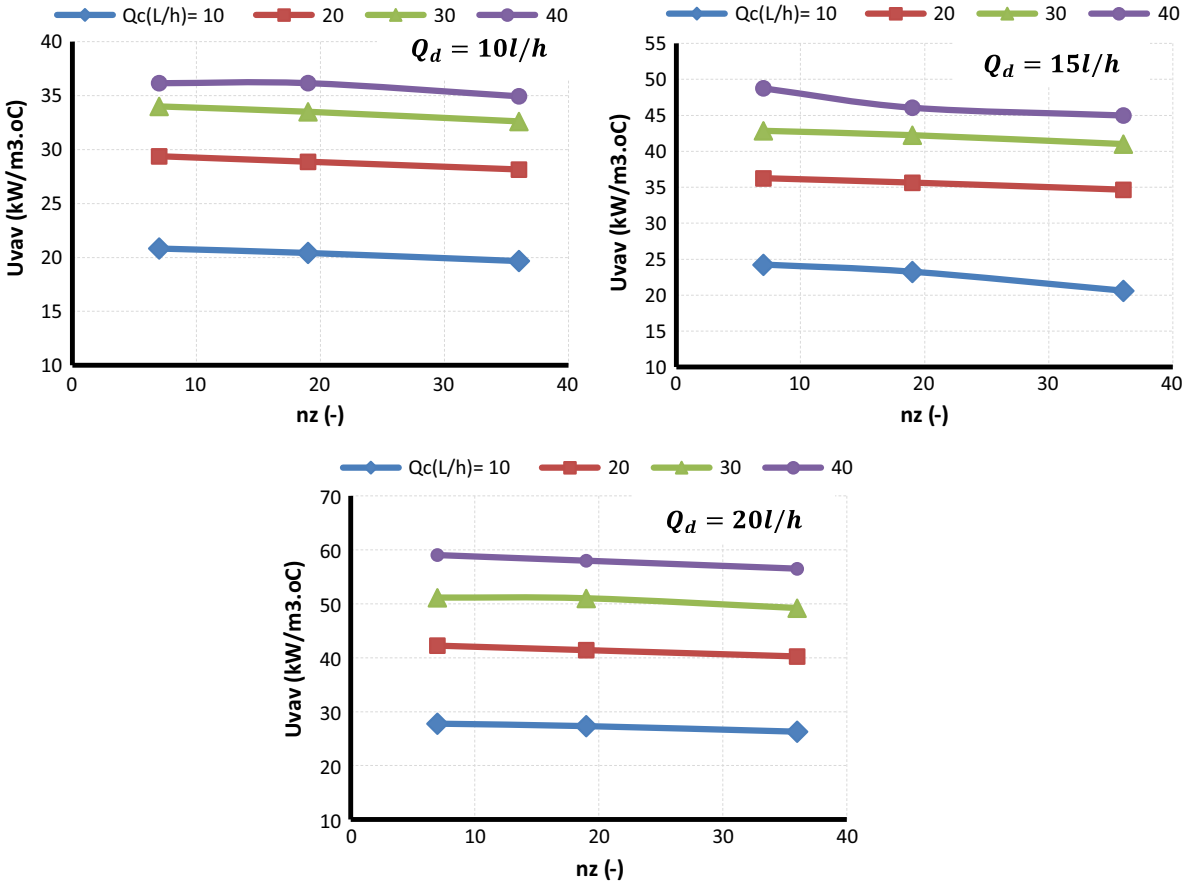

Fig. 3. Variation of the average volumetric heat transfer coefficient with sparger configuration for four different continuous phase flow rates and three different dispersed phase flow rates.

persed phase flow rate, there was only a very slight effect of the sparger configuration on the average volumetric heat transfer coefficient. As shown by Fig. 2, a smaller the drop size results in a higher volumetric heat transfer coefficient. For a constant nozzle diameter, smaller drops will be produced with a lower number of nozzles because of the high dispersed phase velocity at the nozzles, which reduces the drop formation time. In addition, a smaller number of drops is associated with a smaller interfacial heat transfer area. These two effects could be balanced in the present experiments, which are results in a small effect of sparger configuration on the average heat transfer coefficient.

3.2. Effect of continuous flow rate

It was shown above (see Fig. 2) that the continuous phase flow rate significantly affected the average volumetric heat transfer coefficient by altering the initial drop size. The dependency of the average volumetric heat transfer coefficient on the continuous flow rate at three different dispersed flow rates is shown by Fig. 4. From the figures, it is obvious that the average volumetric heat transfer coefficient increases with an increase of the continuous phase flow rate. As justified above, the high continuous phase flow rate means abundant energy is available in the evaporator. With the assumption of no heat loss from the evaporator, the law of conservation of energy implies a high heat transfer rate between the two phases in the evaporator.

In addition, the figure reveals the dependency of the average volumetric heat transfer coefficient on the dispersed phase flow rate. It is obvious that the average heat transfer coefficient increases upon an increase of the dispersed phase flow rate. Also, and as mentioned above, the higher dispersed phase flow rate produces a smaller drop size by affecting the velocity at the sparger. This will lead to increase the heat transfer area and consequently increase the direct contact heat transfer. Furthermore, it is clear [e.g. 27] that the direct contact evaporation in the three-phase spray column heat exchanger exclusively relies on the area of liquid–liquid interface. This area decreases as evaporation progresses and it would reach its minimum value (zero) when the drops have completely evaporated. The internal heat transfer resistance also develops within the drops due to the poor thermal conductivity of the vapour formed. Therefore, the heat exchange rate, and similarly the average volumetric heat transfer coefficient, decreases as evaporation continues and it could be entirely hindered at the end of drop's evaporation.

Fig. 5 shows the effect of the sparger configuration on the average volumetric heat transfer coefficient at three different dispersed phase flow rates. In general, the average volumetric heat transfer coefficient is very slightly decreased by an increase in the number of nozzles in the sparger. This is in agreement with previous observations presented in Fig. 3.

At the same dispersed phase flow rate and nozzle diameter, the larger number of nozzles in the sparger could result in a reduction in the injection velocity of the dispersed phase. Consequently, large drops will be produced due to the large formation time that is initiated by lower pressure drop across the sparger. Fig. 5 reveals the very slight decline in the average volumetric heat transfer coefficient with an increase in the number of nozzles in the sparger that was not clearly shown in Fig. 3.

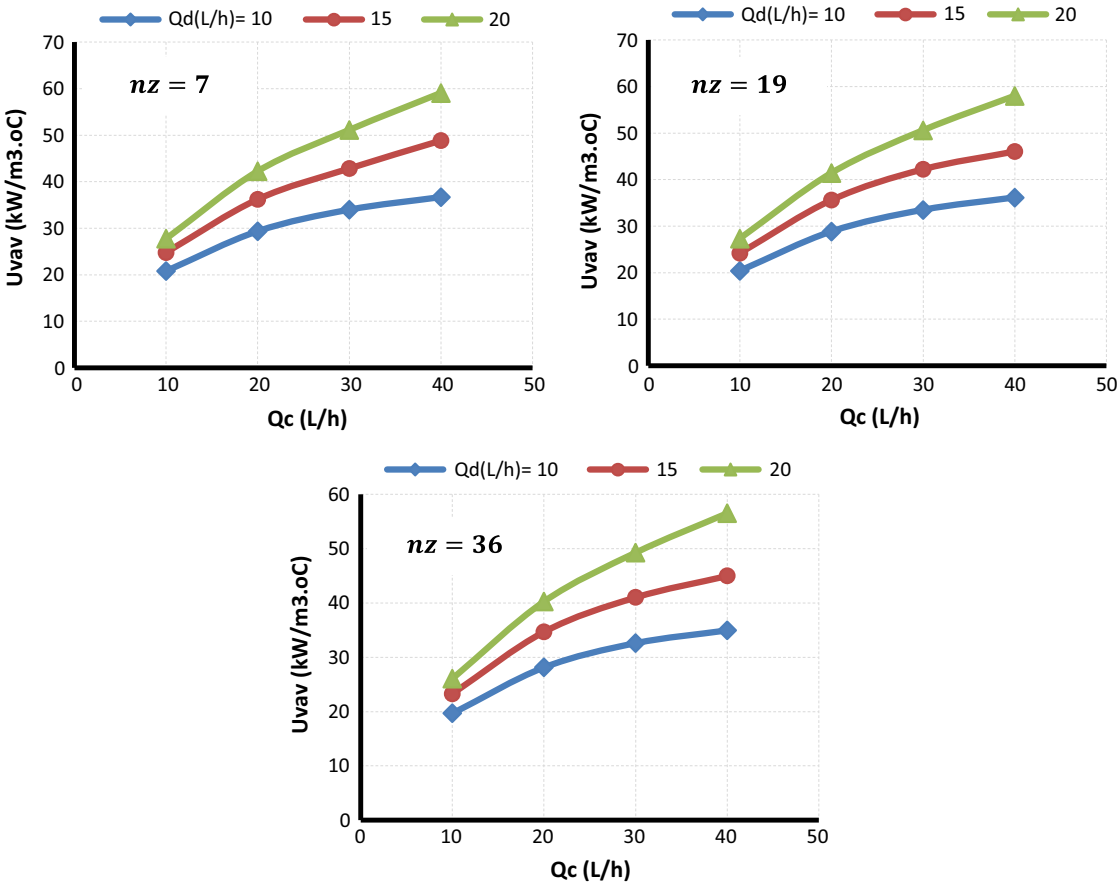

Fig. 4. Variation of the average volumetric heat transfer coefficient with the continuous phase flow rate for three different dispersed phase flow rates and sparger configurations.

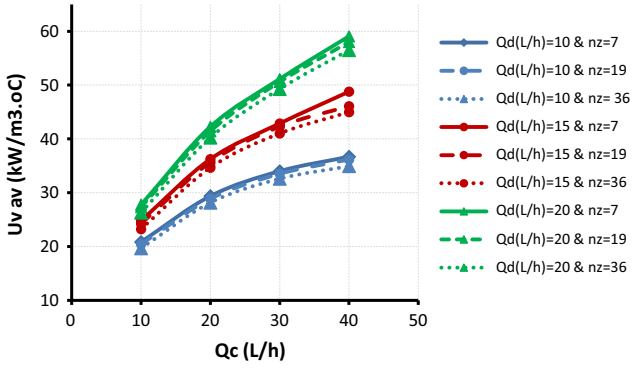

Fig. 5. Effect of the sparger configuration on the variation of the average volumetric heat transfer coefficient with the continuous phase flow rate for three different dispersed phase flow rates.

3.3. Effect of hold-up

Hold-up was calculated depending on the continuous phase height in the exchanger before and after the dispersed phase was injected, using the simple expression:

$$\phi = \frac{L - L_o}{L_o} \tag{6}$$

where L and L_o represent the continuous phase height in the exchanger before and after dispersed phase injected.

It was observed that the hold-up is mainly dependent on the dispersed phase flow rate that causes the change in the continuous phase level in the exchanger [3]. Fig. 6a shows the variation of hold-up with dispersed phase flow rate for three different sparger configurations. An approximately linear relationship between the hold-up and the dispersed phase is obvious, as shown in Fig. 6a. This is consistent across all three configurations considered herein.

Furthermore, the relationship between hold-up and the average volumetric heat transfer coefficient is shown by Fig. 6b, for three different sparger configurations. It is obvious that the higher the hold-up, the higher the average volumetric heat transfer coefficient. This could be due to the fact that the high hold-up means abundant dispersed phase in the exchanger, which enhances the direct contact heat transfer in the exchanger according to the simple energy balance, and as justified above. Again, a very slight effect of sparger configuration on the average volumetric heat transfer coefficient is noted.

3.4. Effect of active height

A direct contact heat exchanger can be operated at different active heights. This height significantly affects the exchanger's cost [1]. Put simply, the active height represents the minimum continuous height that can be used to achieve complete evaporation of the dispersed phase drops. Many parameters, such as the initial drop size, the dispersed phase flow rate, the continuous phase flow rate and exchanger diameter can directly affect the active height.

Fig. 7 shows the variation of the average volumetric heat coefficient with the active height of the direct contact heat exchanger,

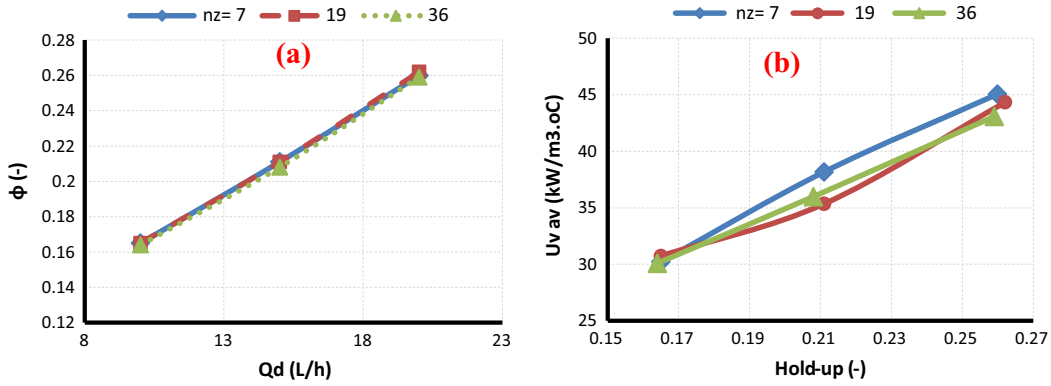

Fig. 6. (a) Hold-up variation with the dispersed phase flow rates for three different sparger configurations. (b) Variation of the average volumetric heat transfer coefficient with hold-up for different sparger configurations.

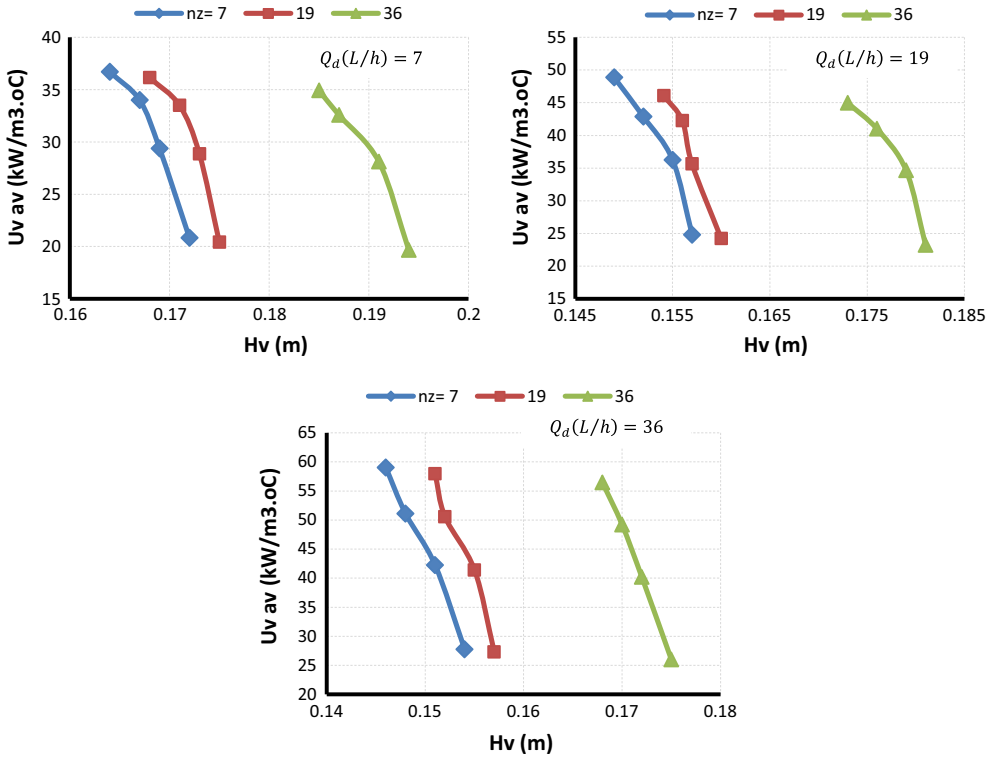

Fig. 7. Variation of the average volumetric heat transfer coefficient with active continuous phase height for three different sparger configurations and dispersed phase flow rates.

for three different sparger configurations. Interestingly, the figure shows that the active height affects the average volumetric heat transfer coefficient. The lower the exchanger active height, the higher is the average volumetric heat transfer coefficient. This could be explained by the fact that the long active height is associated with a slow heat exchange between the contacting fluids hence a reduced average volumetric heat transfer coefficient. No notable impact of the sparger configuration on the average volumetric heat transfer coefficient is clearly shown by the figure, which confirms the previous observation above (see Fig. 3).

4. Conclusions

The average volumetric heat transfer coefficient of a liquid–liquid–vapour direct contact evaporator has been studied experimentally. The impact of different operational parameters, such as the initial drop size, the dispersed phase flow rate, the continuous phase flow rate, the sparger configuration, the hold-up and the exchanger active height on the average volumetric heat transfer coefficient in the evaporator were investigated. According to the results, it can be concluded that a high heat exchange was achieved, especially at the beginning of the direct contact heat transfer process. The heat transfer process was strongly affected by the initial drop size and the progress of evaporation of the drops. The smaller the initial drops size, the higher was the volumetric heat transfer coefficient. The progress of evaporation tends to reduce the liquid–liquid interface within the drop, which controls the heat transfer area, and increases the drops internal heat transfer resistance. Also, both dispersed phase and continuous phase flow rates have positive effects on the average volumetric heat transfer coefficient. No notable impact of the sparger configuration on the average heat transfer coefficient was seen.

In addition, the hold-up is linearly increased with the dispersed phase and it similarly affected the average volumetric heat transfer coefficient.

References

[1] H.B. Mahood, A.N. Campbell, R.B. Thorpe, A.O. Sharif, Heat transfer efficiency and capital cost evaluation of a three-phase direct contact heat exchanger for the utilisation of low-grade energy sources, Energy Convers. Manage. 106 (2015) 101–109.

[2] H.B. Mahood, R.B. Thorpe, A.N. Campbell, A.O. Sharif, Experimental measurements and theoretical prediction for the transient characteristic of a three-phase direct contact condenser, J. Appl. Therm. Eng. 87 (2015) 161–174.

[3] G.L. Bauerle, R.C. Ahlert, Heat transfer and holdup phenomena in spray column, Ind. Eng. Chem. Process Des. Dev. 4 (2) (1965) 225–230.

[4] S.B. Plass, H.R. Jacobs, R.F. Boehm, Operational characteristics of a spray column type direct contact contactor preheater, AIChE Symp. Ser.-Heat Transfer 75 (189) (1979) 227–234.

[5] P. Goodwin, M. Coban, R. Boehm, Evaluation of the flooding limits and heat transfer of a direct contact three phase spray column, in: National Heat Transfer Conference, Denver, August, 1985, pp. 1–5.

[6] J. Siqueiros, O. Bonilla, An experimental study of a three-phase, direct-contact heat exchanger, Appl. Therm. Eng. 19 (5) (1999) 477–493.

[7] M. Song, A. Steiff, P.-M. Weinspach, The analytical solution for a model of direct contact evaporation in spray columns, Int. Commun. Heat Mass Transfer 23 (2) (1996) 263–272.

[8] Z. Peng, W. Yiping, G. Cuili, W. Kun, Heat transfer in gas–liquid–liquid three-phase direct-contact exchanger, Chem. Eng. J. 84 (3) (2001) 381–388.

[9] Y. Wang, H. Fu, Q. Huang, Y. Cui, Y. Sun, L. Jiang, Experimental study of direct contact vaporization heat transfer on *n*-pentane–water flowing interface, Energy 93 (2015) 854–863.

[10] S. Sideman, G. Hirsch, Y. Gat, Direct contact heat transfer with change phase: effect of the initial drop size in three-phase heat exchanger, AIChE J. 11 (6) (1965) 1081–1087.

[11] P. Battya, V.R. Raghavan, K.N. Seetharamu, Parametric analysis of direct contact sensible heat transfer in spray column, Lett. Heat Mass Transfer 9 (4) (1982) 265–276.

[12] K.L. Core, J.C. Mulligan, Heat transfer and population characteristics of dispersed evaporating droplets, AIChE J. 36 (8) (1990) 1137–1144.

[13] S.M. Summers, C.T. Crowe, One-dimensional numerical model for a spray column heat exchanger, AIChE J. 37 (11) (1991) 1673–1679.

[14] R.A. Brickman, R.F. Boehm, Maximizing three-phase direct contact heat exchanger output, Num. Heat Transfer, Part A: Appl. 26 (3) (1994) 287–299.

[15] T. Coban, R. Boehm, Performance of a three-phase, spray-column, direct-contact heat exchanger, J. Heat Transfer 111 (1) (1989) 166–172.

[16] H.R. Jacobs, M. Golafshani, Heuristic evaluation of the governing mode of heat transfer in a liquid–liquid spray column, J. Heat Transfer 111 (3) (1989) 773–779.

[17] L. Tadrist, J. Sun, R. Santini, J. Pantaloni, Heat transfer with vaporization of a liquid by direct contact in another immiscible liquid: experimental and numerical study, J. Heat Transfer 113 (3) (1991) 705–713.

[18] Y. Shimizu, Y.H. Mori, Evaporation of single liquid drops in an immiscible liquid at elevated pressure: experimental study with *n*-pentane and R113 drops in water, Int. J. Heat Mass Transfer 31 (9) (1988) 1843–1851.

[19] Y.H. Mori, An analytic model of direct-contact heat transfer in spray-column evaporators, AIChE J. 37 (4) (1991) 539–546.

[20] H.B. Mahood, A.O. Sharif, S.A. Hossini, R.B. Thorpe, Analytical modelling of a spray column three-phase direct contact heat exchanger, ISRN Chem. Eng. (2013), http://dx.doi.org/10.1155/2013/457805 457805.

[21] Y. Jian, Q. Huang, Y. Wang, Y. Cui, H. Fu, The effect of Dixon rings on direct contact evaporative heat transfer performance, Appl. Therm. Eng. 87 (2015) 336–343.

[22] H.B. Mahood, A.O. Sharif, S. Al-aibi, D. Hwakis, R.B. Thorpe, Analytical solution and experimental measurements for temperatures distribution prediction of three-phase direct contact condenser, J. Energy 67 (2014) 538–547.

[23] H.B. Mahood, A.O. Sharif, R.B. Thorpe, Transient volumetric heat transfer coefficient prediction of a three-phase direct contact condenser, J. Heat Mass Transfer 51 (2) (2015) 165–170.

[24] H.B. Mahood, A.N. Campbell, R.B. Thorpe, A.O. Sharif, Experimental measurements and theoretical prediction for the volumetric heat transfer coefficient of a three-phase direct contact condenser, Int. Commun. Heat Mass Transfer 66 (2015) 180–188.

[25] H.B. Mahood, A.N. Campell, A.O. Sharif, R.B. Thorpe, Heat transfer measurement in a three-phase direct contact condenser under flooding conditions, Appl. Therm. Eng. 95 (2016) 106–114.

[26] S. Sideman, Y. Tailtel, Direct-contact heat transfer with change of phase: evaporation of drops in an immiscible liquid medium, Int. J. Heat Mass Transfer 7 (11) (1964) 1273–1289.

[27] S. Sideman, Y. Gat, Direct contact heat transfer with change of phase: spray column studies of a three-phase heat exchanger, AIChE J. 12 (2) (1966) 296–303.